To appear in *Vehicle System Dynamics*
Vol. 00, No. 00, Month 20XX, 1–22

RESEARCH ARTICLE

Feedback brake distribution control for minimum pitch

Davide Tavernini[a] * , Efstathios Velenis[b] and Stefano Longo[b]

[a] *Centre for Automotive Engineering, University of Surrey, Guildford, United Kingdom;*
[b] *Advanced Vehicle Engineering Centre, Cranfield University, Cranfield, United Kingdom;*

()

The distribution of brake forces between front and rear axles of a vehicle is typically specified such that the same level of brake force coefficient is imposed at both front and rear wheels. This condition is known as 'ideal' distribution and it is required to deliver the maximum vehicle deceleration and minimum braking distance. For subcritical braking conditions, the deceleration demand may be delivered by different distributions between front and rear braking forces. In this research we show how to obtain the optimal distribution which minimises the pitch angle of a vehicle and hence enhances driver subjective feel during braking. A vehicle model including suspension geometry features is adopted. The problem of the minimum pitch brake distribution for a varying deceleration level demand is solved by means of a model predictive control technique. To address the problem of the undesirable pitch rebound caused by a full-stop of the vehicle, a second controller is designed and implemented independently from the braking distribution in use. An extended Kalman filter is designed for state estimation and implemented in a high fidelity environment together with the model predictive control strategy. The proposed solution is compared with the reference 'ideal' distribution as well as another previous feed-forward solution.

Keywords: Pitch, anti-dive, suspension geometry, brake distribution, model predictive control, heave estimation.

1. Introduction

The ratio between front and rear axle brake forces (brake force distribution) represents a critical characteristic of a vehicle as it may affect vehicle handling stability. In particular, in an emergency braking situation, locking of the rear wheels prior to the front leads to an unstable and hazardous operating condition. In order to prevent the above critical situation, the brake force distribution needs to be properly specified. In this way legal requirements with regards to vehicle handling can be satisfied. An 'ideal' brake force distribution is defined in the literature [1], resulting from the requirement that front and rear tyres generate equal amounts of braking force normalized by the respective normal load (referred to as equal skid resistance). It can be easily shown that this 'ideal' distribution leads to minimum braking distance as all tyres will operate at the peak of adhesion simultaneously. Calculation of the 'ideal' distribution for different levels of vehicle deceleration includes the weight transfer effect. Vehicle brake systems are typically tuned either with a fixed distribution, or a varying distribution using proportioning valves for the rear (or sometimes front) brakes in order to approximate

*Corresponding author. Email: d.tavernini@surrey.ac.uk

the 'ideal' distribution curve. The Electronic Braking force Distribution system (EBD) actively varies the ratio between front and rear brake forces using the Anti-lock braking system (ABS) actuators to better follow the 'ideal' curve [2].

The emergence of Hybrid-Electric Vehicles (HEV) in the last decades and the development of regenerative braking systems to recuperate energy during braking using the electric powertrain as a generator has motivated further research into the brake force distribution strategy. In particular, there are several approaches in the literature proposing a deviation from the 'ideal' braking distribution [3], [4], [5], [6] in favor of the efficiency of regeneration. Integration of regenerative braking in HEV vehicles is made possible through the use of brake-by-wire friction systems. They can actively adjust the brake force generated by friction brakes in individual wheels, to allow blending with electric motor braking. Regenerative braking is typically restricted to subcritical braking at low decelerations in order to avoid instability [7].

Vehicles employing brake-by-wire systems result in overactuated systems, since the same deceleration level (for subcritical braking scenarios) can be met with different combination of front and rear braking force distribution. Assuming braking events with the tyres operating away from their saturation point, in this work we show how to take advantage of this actuators' redundancy and propose a brake force distribution optimisation to achieve enhanced driver and passengers subjective feel during braking. The parameter that has been associated to this aspect is the pitch angle of the vehicle, which occurs during braking and dynamic load shift from the rear to the front wheels. Typically, control of the pitch angle falls in the domain of active suspensions [8], [9]. However, it is well known that the suspension geometry, and specifically the location of the front and rear pitch centres and corresponding anti-dive and anti-lift properties have an effect on the vehicle vertical and pitch motions during longitudinal acceleration/deceleration [10], [11], [12], which depends on the ratio of front to rear longitudinal tyre forces. Specific anti- (i.e. anti-dive and anti-lift) features are defined as target in the suspension design process to passively control pitch and heave of a vehicle. Here we propose to use actively varying braking force distribution in order to minimise pitch during braking, avoiding additional actuators for an active suspension system. The connection between a stationary pitch angle and driver feel follows the same line of reducing roll angle during cornering, without cancelling it completely. Systems to control roll angle are employed for improvement of vehicle handling as well as driver comfort, and result in a roll angle reduction [13].

In [14] an alternative distribution to the 'ideal' one was proposed, where the rear brake force is exploited at a higher level, yet lying in a stable area (varying with deceleration level) for the vehicle handling. By means of experimental results the effect of vehicle pitch reduction during braking was also pointed out and presented as an interesting side effect to an improved vehicle dynamics together with enhancing stability while braking into a curve. Moreover it was stated that the effect of the distribution on the vehicle pitch "...would impress a driver with vehicle grabbing or holding the road surface during braking.". This, together with the experimental tests performed in [15] confirms that, although driver comfort is mostly associated with body accelerations, a combination of pitch and heave motions from the chassis could lead to more or less reassuring braking for an every-day driver, and thus enhance his subjective feel.

In order to develop the control strategy we first introduce a vehicle model with longitudinal, vertical and pitch dynamics that incorporates the front and rear suspension pitch centre locations and anti-lift/dive geometry, which allows the model to capture the effect of longitudinal force distribution between front and rear axles on the chassis dynamics. The model finds its origin in [12]. It has been modified and simplified in

the suspension dynamics and geometry definition, but also properly augmented with a longitudinal jerk equation, for control design.
In [15] the authors presented a feed-forward strategy to address the minimum pitch brake distribution problem. A map of vehicle deceleration to optimal force distribution was obtained by means of a set of static optimisation for a vehicle in quasi-static motion conditions. Both simulation and experimental results comparing the implementation of minimum pitch strategy with the 'ideal' EBD brake torque distribution were provided. This easily implementable solution has the advantage to be computationally inexpensive and also easily certifiable because no optimisation processes are solved on line. It can be applied on a real vehicle with reduced requirement of measurement from the vehicle and included in production vehicles' control architectures. On the other hand it has the disadvantage of guaranteeing the optimality only under certain conditions (e.g. quasi-static conditions) and the underachievement of the driver demand (in terms of deceleration) is not monitored or corrected in any way. To solve the same problem of minimising pitch while braking, as well as reducing the pitch rebound caused by a full-stop braking, in this research we address the design of two feedback controllers. They are based on a model predictive control (MPC) approach that allows to impose constraints both on states and inputs. The unconstrained case for the same case study, was presented by the authors again in [15]. Two LQR (Linear Quadratic Regulator) controllers were shown to properly control the vehicle in simulations employing a simple vehicle model as the plant, but revealed their limits for a real implementation due their unconstrained nature.
The problem of a hard full-stop braking and the consequent pitch rebound, that is overall subjectively considered an uncomfortable effect for an everyday driver, has been previously addressed for a fully electric vehicle in [16] by means of a PI closed-loop controller for pitch angle (with a zero pitch target) that generates an acceleration target as input, delivered employing a slip-control. Braking action is considered as an overall action on the vehicle and thus pitch control is achieved by reducing the acceleration of the vehicle. In the current paper, as for [15], the rebound problem is solved through a full-state feedback controller for two independent front/rear input forces as an extension of the other controller already designed for minimum pitch during braking. In order to provide the necessary signals for the full-state feedback controllers an extended Kalman filter (EKF) is developed and tested in combination with the MPC approach in a high fidelity environment. Examples of EKF based MPC are provided in [17] and [18]. In this last study in particular output from the model predictive controller were directly applied as inputs to the extended Kalman filter.

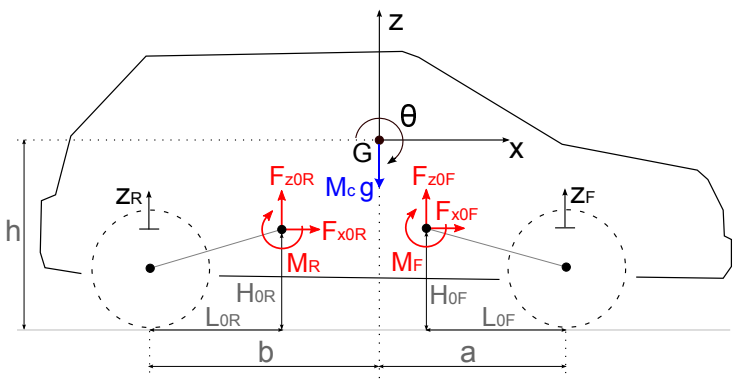

Figure 1. Chassis free body diagram. X-Z plane.

The same approach is adopted in our research where observer and model predictive controller become a single control entity strongly interconnected. An example of pitch angle estimation algorithm can be found in [19] where kinematic based observer were adopted to estimate pitch as well as roll vehicle angles. Our research work proposes instead a model-based observer able to estimate a wide range of vehicle states such as pitch, heave and heave rate from a reduced number of measurement, without the employment of expensive sensors. Literature on pitch angle estimation appears to be very limited whereas for the heave motion case the authors are not aware of any study.

2. VEHICLE MODELING

The model employed in this study is a single-track pitch-plane model, with each of the front and rear wheels accounting for equal contributions of left and right wheels of the respective axle of the actual vehicle. Lateral dynamics, roll and yaw motion and wheel rotation dynamics are herein neglected.
Chassis dynamics are described in terms of pitch angle and heave translation (i.e. vertical motion), namely θ and z. In addition, longitudinal motion in terms of speed and position on the road is considered.
The longitudinal dynamics of the vehicle is described by the standard equation:

$$\ddot{x} = \frac{1}{M}(\mu_R \; F_{zR} + \mu_F \; F_{zF}), \tag{1}$$

where F_{zi} with $i = R, F$ are rear and front vertical loads on the tyres, and μ_i with $i = R, F$ are the tyre brake force coefficients, M is the total mass of the vehicle, and x is the travelled distance. The free body diagram of the chassis (sprung mass) represented in Fig.1 is now analysed.
The model includes suspension dynamics and geometry. Torsional springs and dampers are employed and represented by suspension torques M_i with $i = R, F$. Reaction forces (vertical and longitudinal), namely F_{z0i} and F_{x0i} are applied at the suspension pivots. The front and rear suspension pivot points (pitch centres) are assumed to be fixed irrespective of chassis pitch and heave motions.
Rear and front chassis vertical displacements and rates, namely z_i and $\dot{z}_i$ with $i = R, F$

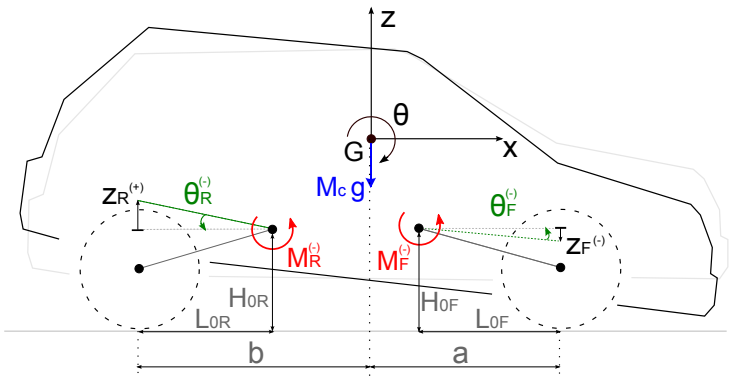

Figure 2. Suspension rotation and torque calculation. X-Z plane. Sign convention is explained by means of an example case of pitch and heave. The choice is that a positive pitch angle generates negative suspension rotations and negative suspension reaction moments and rotations are defined so that they are positive clock-wise.

are computed with respect to pitch and heave dynamics:

$$z_R = \tan(\theta)\ b + z, \tag{2}$$

$$\dot{z}_R = (1 + \tan(\theta)^2)\ \dot{\theta}\ b + \dot{z}, \tag{3}$$

$$z_F = -\tan(\theta)\ a + z, \tag{4}$$

$$\dot{z}_F = -(1 + \tan(\theta)^2)\ \dot{\theta}\ a + \dot{z}, \tag{5}$$

where θ and $\dot{\theta}$ are chassis pitch angle and rate, z and $\dot{z}$ are the chassis heave displacement and rate, a and b provide the longitudinal distance of the centre of mass G from front and rear tyre contact point respectively.
The front and rear suspension rotation angles and rates θ_i and $\dot{\theta}_i$ with $i = R, F$ shown in Fig.2 can be derived from (2-5):

$$\theta_R = -\arctan(\frac{z_R}{L_{0R}}), \tag{6}$$

$$\dot{\theta}_R = -\frac{1}{1 + (\frac{z_R}{L_{0R}})^2}\ \frac{\dot{z}_R}{L_{0R}}, \tag{7}$$

$$\theta_F = \arctan(\frac{z_F}{L_{0F}}), \tag{8}$$

$$\dot{\theta}_F = \frac{1}{1 + (\frac{z_F}{L_{0F}})^2}\ \frac{\dot{z}_F}{L_{0F}}. \tag{9}$$

Suspension torques M_i can be computed as the sum of a static term and torque due to suspension deflection (i.e. rotation) and rate of deflection:

$$M_R = \frac{a}{a+b}\ M_c\ g\ L_{0R} + k_R\ \theta_R + c_R\ \dot{\theta}_R, \tag{10}$$

$$M_F = -\frac{b}{a+b}\ M_c\ g\ L_{0F} + k_F\ \theta_F + c_F\ \dot{\theta}_F. \tag{11}$$

L_{0i} with $i = R, F$ are the longitudinal distances between contact points and suspension pivots, k_i and c_i with $i = R, F$ are suspension torsional stiffness and damping coefficients respectively, M_c is the sprung mass of the vehicle.
From equilibrium of moments around the centre of mass in Fig.1 we obtain the equation

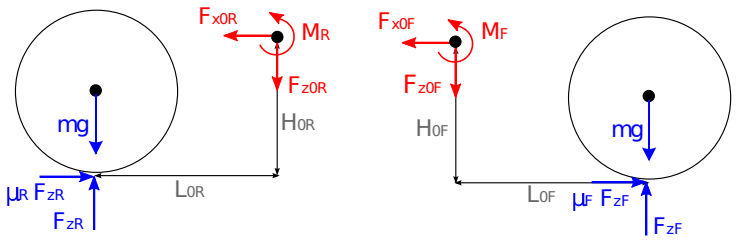

Figure 3. Rear and front wheel-suspension subsystems free body diagrams, X-Z plane.

for pitch acceleration $\ddot{\theta}$:

$$\begin{aligned}\ddot{\theta} =& \frac{1}{J}(M_F + M_R + F_{z0R}\ (b - L_{0R}) - F_{z0F}\ (a - L_{0F}) \\ & - F_{x0R}\ (h - H_{0R}) - F_{x0F}\ (h - H_{0F})).\end{aligned} \tag{12}$$

The vertical acceleration of the chassis $\ddot{z}$ is given by

$$\ddot{z} = \frac{1}{M_c}\ (F_{z0R} + F_{z0F}) - g. \tag{13}$$

Next, we consider separately the free body diagrams of rear and front wheel-suspension systems in Fig.3.
From the longitudinal equilibrium of forces in Fig.3 it turns out that the longitudinal reaction forces F_{x0i} can be computed as:

$$F_{x0R} = \mu_R\ F_{zR}, \qquad F_{x0F} = \mu_F\ F_{zF}. \tag{14}$$

Similarly for F_{z0i} and the equilibrium of vertical forces.

$$F_{z0R} = F_{zR} - m\ g, \qquad F_{z0F} = F_{zF} - m\ g, \tag{15}$$

where m is both rear and front unsprung masses.
At this point from the equilibrium of moments around suspension pivots and the definition of suspension torques in (10)-(11) vertical loads F_{zi} can be calculated as follows:

$$F_{zR} = \frac{M_R + m\ g\ L_{0R}}{-\mu_R\ H_{0R} + L_{0R}}, \tag{16}$$

$$F_{zF} = \frac{M_F - m\ g\ L_{0F}}{-\mu_F\ H_{0F} - L_{0F}}. \tag{17}$$

The effect of unsprung masses m on vertical loads F_{zi} is taken into account, added as a simple static term on both axles, neglecting the small impact that unsprung masses load transfer would have on the normal loads. Since this model includes effects of braking distribution between front and rear axles, the anti- features quantities can be computed. In particular, anti-dive accounts for compression of the front suspension during braking and thus squat of the chassis in the front. Similarly anti-lift considers extension of the rear suspension that corresponds on lift of the rear part of the chassis. These two effects

Table 1. Parameters of the vehicle model.

Parameter	Symbol	Value
Gravity (m/s^2)	g	9.81
Total Mass (kg)	M	1946
Sprung Mass (kg)	M_c	1695
Unsprung Mass (kg)	m	125.5
Total pitch inertia (kg m^2)	J	2500
Height of CoM (m)	h	0.75
Distance of CoM from rear (m)	b	1.544
Distance of CoM from front (m)	a	1.121
Rear susp. stiffness (Nm/rad)	k_R	13306
Front susp. stiffness (Nm/rad)	k_F	37966
Rear susp. damping (Nm/rad s)	c_R	2185.8
Front susp. damping (Nm/rad s)	c_F	3982.2
Rear pivot height (m)	H_{0R}	0.15554
Front pivot height (m)	H_{0F}	0.035431
Rear pivot from rear wheel (m)	L_{0R}	0.53484
Front pivot from front wheel (m)	L_{0F}	0.7057

strongly influence pitch and heave characteristics of the vehicle according to the distribution of the brake force.
Anti-dive and anti-lift percentages [11] can be computed respectively as:

$$F_{aD} = \frac{F_F}{F_F + F_R} \frac{H_{0F}}{L_{0F}} \frac{a+b}{h} \ \%, \tag{18}$$

$$R_{aL} = \frac{F_R}{F_F + F_R} \frac{H_{0R}}{L_{0R}} \frac{a+b}{h} \ \%, \tag{19}$$

where:

$$F_R = \mu_R \ F_{zR}, \qquad F_F = \mu_F \ F_{zF}. \tag{20}$$

Suspension parameters for the proposed geometry included in the presented model have been identified by means of the Matlab®'s Identification Toolbox employing data from a high fidelity model simulation (i.e. IPG® CarMaker) and are reported in Tab.1.

3. FEEDBACK CONTROLLER DESIGN AND FORMULATION

In the case of a brake distribution strategy, an objective that is difficult to totally fulfil is the demanded deceleration level for a specific driver effort on the brake pedal. For this aim an acceleration feedback is required. At the same time other targets need to be set to achieve the minimum-pitch distribution, in terms of vehicle pitch and heave motion mainly, being these two chassis motions strongly coupled, when selecting different longitudinal forces distribution.
The choice is thus to employ a full-state feedback controller in order to monitor the different aspects (state variables) of the vehicle dynamics and to set specific targets also

inferred from the quasi-static analysis presented in [15]. Moreover the feedback approach is the only one that allows to manage model uncertainties such as vehicle weight or, like in this case, suspension geometry, that directly influence the vertical loads calculation, unlike a feed-forward one that requires to be adjusted when some of the conditions for which the control action has been derived, change. Two problems are considered herein: the minimum-pitch distribution during braking and the reduction of the pitch rebound that occurs in a full-stop brake. This rebound event is due to a longitudinal acceleration step response from a predefined value to zero (where no braking forces are applied). When this happens, the vehicle pitch angle is recovered in a very short time and thus the vehicle inertia is enough to generate a rebound and thus a negative pitch when the vehicle comes to a full-stop. The two problems are considered as two different challenges and therefore are dealt with employing two different controllers (in terms of states' targets). The full-stop controller is designed to be completely independent from the braking distribution in use. Besides, employing the same feedback technique, the computation of the optimal brake force distribution for minimum pitch in steady braking is also addressed. This is presented as an alternative solution to a feed-forward one.
The system considered for the feedback control design is an extension of the one presented in Section 2. The normalized longitudinal forces are not directly controlled this time, but this is done through their time-derivatives (22). This modification was a necessary step since a longitudinal jerk equation (21) has been introduced.

$$\dot{a}_x = f(\mu_R, \mu_F, \mu_{R_{rate}}, \mu_{F_{rate}}), \tag{21}$$

$$\dot{\mu}_R = \mu_{R_{rate}}, \qquad \dot{\mu}_F = \mu_{F_{rate}}. \tag{22}$$

Considering the longitudinal acceleration a_x as a state variable allows us to define an acceleration target for the controller to pursue. In this way the closed-loop controller includes acceleration in the feedback loop.
The state vector for the new formulation becomes $\mathbf{x} = [a_x, \theta, \dot{\theta}, z, \dot{z}, \mu_R, \mu_F]$ and the input vector $\mathbf{u} = [\mu_{R_{rate}}, \mu_{F_{rate}}]$.
In the following sections the design of the two different feedback controllers is presented. They are developed separately and are independent in the implementation. For each model state a specific target is defined and a weight coefficient is introduced in order to tune the controller performance. High weight means that more effort in terms of control action is allocate to achieve the correspondent target. The linear quadratic regulator (LQR) approach has been already presented and discussed in [15]. In the current study an MPC approach is adopted, it guarantees the feasibility of the computed control action since physical actuators limits can be accounted for in the formulation, unlike the LQR solution, and state constraints can be also put in place to avoid solutions that go beyond the physical possibilities of the considered vehicle (like normalised longitudinal forces that become states in the current formulation).

3.1. *Minimum pitch force distribution in steady braking*

The aim of the MPC_{mp} (i.e. MPC for minimum pitch) controller is to modulate the braking forces during a deceleration event, whose level is imposed by the driver braking action, in order to minimise the vehicle pitch angle. In the specific case study presented in this research the target for acceleration is set to $a_{x_T} = -0.5\text{g}$ and a high weight is imposed, pitch target is $\theta_T = 0\text{rad}$, again imposing a high weight. Heave target is

defined from the analysis of previous results from EBD and quasi-static (QS) Map [15]: $z_T = -0.05$m. The reason for this is that pitch and heave are strongly coupled in the model so that an unrealistic target for z does not allow the controller to achieve the minimum pitch possible. A smaller (in relative terms) weight is used in this case, to leave more emphasis on the vehicle pitch. A small weight is adopted for pitch rate and heave rate. For normalized longitudinal forces (that this time are systems states) the target is chosen as the quasi-steady state value found employing EBD (i.e. $\mu_{R_T} = \mu_{F_T} = -0.5$), but an almost null weight is applied to leave the MPC_{mp} controller to choose their values freely.

3.2. *Pitch rebound overshoot in a full-stop*

In the final part of the braking event the MPC_{fs} (i.e. MPC for full-stop) controller is applied, simply switching from one to the other as soon as the longitudinal vehicle velocity drops below a predefined threshold $V_{th} = 1$m/s.
This MPC addresses the problem of the problem of a hard full-stop and the pitch rebound of the chassis when the vehicle comes to a full-stop. This aspect of the braking dynamics was already pointed out in [15] where experimental results highlight what already emerged from simulations. When the vehicle comes to a full-stop the pitch angle, that has been reached during the previous braking, is quickly recovered resulting in an rebound before returning to zero. In this case the hard full-stop leading to the rebound is objectively considered as uncomfortable and experienced drivers try to avoid it modulating the braking effort on the brake pedal in the very end of the braking manoeuvre. Employing the same model as for MPC_{mp}, some weights (i.e. Q and R matrices) and state targets $\mathbf{x}_T$ are varied to pursue a new aim: obtaining the smoothest braking to a full-stop in terms of vehicle pitch angle. In particular, with respect to MPC_{mp}, the weight on longitudinal acceleration is drastically reduced to almost zero, whereas weights on normalized forces are increased to a medium weight level. μ_{R_T}, μ_{F_T} are also set to a very small value in order to maintain a minimum braking action and thus guarantee a vehicle full stop. This adjustment is also performed to reduce the acceleration step as much as possible, reducing the braking action before the full-stop. Small weights have been tested as well, with unnoticeable difference in the results. At the same time, heave motion target is changed to zero to match the condition of a stationary vehicle.
Details on MPC theory are now provided.

The continuous-time non-linear system:

$$\dot{\mathbf{x}}(t) = f(\mathbf{x}(t), \mathbf{u}(t)), \qquad \mathbf{y}(t) = g(\mathbf{x}(t), \mathbf{u}(t)), \tag{23}$$

where $\mathbf{x}$, $\mathbf{u}$, $\mathbf{y}$ are state, input and output respectively, is linearised around an equilibrium point ($\mathbf{x}^{ss}$, $\mathbf{u}^{ss}$, $\mathbf{y}^{ss}$). For this specific application the conditions are derived from the quasi-steady-state formulation derived in [15] using as input the deceleration level demand. The system is always linearised around a condition based on the acceleration target.
This leads to the linearised continuous system:

$$\dot{\tilde{\mathbf{x}}}(t) = A\ \tilde{\mathbf{x}}(t) + B\ \tilde{\mathbf{u}}(t), \qquad \tilde{\mathbf{y}}(t) = C\ \tilde{\mathbf{x}}(t) + D\ \tilde{\mathbf{u}}(t) \tag{24}$$

where A, B, C and D represent the continuous jacobian matrices to perform the linearisation. The obtained continuous system is then transformed into a discrete-time one

employing an exact discretisation technique [20] to calculate the discrete jacobian matrices A_d, B_d, C_d and D_d:

$$\tilde{\mathbf{x}}_{k+1} = A_d\ \tilde{\mathbf{x}}_k + B_d\ \tilde{\mathbf{u}}_k, \qquad \tilde{\mathbf{y}}_k = C_d\ \tilde{\mathbf{x}}_k + D_d\ \tilde{\mathbf{u}}_k. \tag{25}$$

where $\tilde{\mathbf{x}} = \mathbf{x} - \mathbf{x}^{ss}$, $\tilde{\mathbf{u}} = \mathbf{u} - \mathbf{u}^{ss}$, $\tilde{\mathbf{y}} = \mathbf{y} - \mathbf{y}^{ss}$.
In the current study the matrix D is assumed to be zero to avoid feed through term and C is selected to be the identity matrix I^n (full-state feedback).
The MPC problem is:

$$\text{minimise} \qquad J = \sum_{j=0}^{N-1} \begin{bmatrix} \mathbf{x}_j^{err} \\ \mathbf{u}_j \end{bmatrix}^T \begin{bmatrix} Q_d & S_d \\ S_d^T & R_d \end{bmatrix} \begin{bmatrix} \mathbf{x}_j^{err} \\ \mathbf{u}_j \end{bmatrix} \tag{26}$$

$$\text{subject to} \qquad \mathbf{x}_0^{err} = \mathbf{x}_{current}^{err}, \tag{27}$$

$$\tilde{\mathbf{x}}_{j+1} = A_d\tilde{\mathbf{x}}_j + B_d\tilde{\mathbf{u}}_j\ \ j = 0, 1..N-1, \tag{28}$$

$$\tilde{\mathbf{x}}_j^{\min} \leq \tilde{\mathbf{x}}_j \leq \tilde{\mathbf{x}}_j^{\max}\ \ j = 0, 1..N-1, \tag{29}$$

$$\tilde{\mathbf{u}}_j^{\min} \leq \tilde{\mathbf{u}}_j \leq \tilde{\mathbf{u}}_j^{\max}\ \ j = 1, 2..N, \tag{30}$$

where $\mathbf{x}^{err} = \mathbf{x}_C - \mathbf{x}^{ss} - (\mathbf{x}_T - \mathbf{x}^{ss}) = \mathbf{x}_C - \mathbf{x}_T$ represents the error between the current states and the imposed target value. N is the prediction horizon.
Equation (27) is used to set this initial state to the current one, (29) and (30) are inequality constraints that basically enforce states and control inputs to lay within predefined boundaries.
In particular for this MPC application (29) and (30) become:

$$\mu_{\min} \leq \mu_i \leq \mu_{\max} \qquad i = F, R \tag{31}$$

$$\dot{\mu}_{\min} \leq \dot{\mu}_i \leq \dot{\mu}_{\max} \qquad i = F, R \tag{32}$$

where μ_i and $\dot{\mu}_i$ represents both front and rear normalized longitudinal forces and rate of variation of forces respectively. The quadratic program (QP) problem in the MPC formulation is solved by an active-set method via the Matlab® solver `quadprog`.
Being able to impose constraints on the state variables offers an important advantage. Since the MPC_{fs} (i.e. full-stop controller) has to lead the vehicle to a full-stop as a main target, this condition can be guaranteed by setting appropriate upper limit (small negative values) for the braking forces so that a minimum deceleration action is always present on the vehicle. Furthermore for the MPC_{mp} the control of the longitudinal normalized forces is constrained to stay within physical limits for the vehicle tyres.

4. STATE ESTIMATION FOR CONTROLLERS FEEDBACK

The MPC presented in section 3 is a full-state feedback controller. This means that, at every time step, signals for all the states need to be provided. Although vehicle pitch angle can be measured using dual-GPS antenna as shown in [15], other signals such as heave and forces are difficult or expensive to measure. Furthermore, a measured signal is most of the time noisy and it requires to be properly filtered before employing it for

feedback control. Another possibility is to estimate the states that are used by the closed-loop controller. Kinematic-based observers can be used for this purpose and an example is presented in [19] where they are adopted to estimate vehicle pitch as well as roll angles. As far as the authors are aware, there is no literature for the estimation of the heave motion and its rate of variation. For these reasons the choice in this study is to employ the same mathematical model used for the MPC controllers. A single model-based observer has been selected for this application rather then relying on a combination of different observers for the different states.
In particular, a Kalman filter [21] is adopted as it provides an optimal estimate, minimising the mean value of the sum of the errors with respect to the measurements.
The non-linear vehicle model employed for MPC is considered again. For this reason the extended Kalman filter, rather than the linear version needs to be used.
The system is linearised and discretised with an appropriate sampling time. The linearisation point this time is represented by the estimated states at the previous step.

4.1. *Filter design*

The model considered for the MPC formulation is further extended including the longitudinal vehicle velocity in the state vector. This in fact becomes $\mathbf{x} = [a_x, \theta, \dot{\theta}, z, \dot{z}, \mu_R, \mu_F, u]$, whereas the input vector remains $\mathbf{u} = [\mu_{R_{rate}}, \mu_{F_{rate}}]$.
The current implementation of the filter assumes three different measurements $\mathbf{y}_{meas} = [a_x, \ddot{\theta}, u]$ from the vehicle, namely the longitudinal acceleration, the pitch rate and the longitudinal velocity. The first two are readily available through a standard IMU (Inertial Measurement Unit) including accelerometers and gyroscopes. With regards to the vehicle velocity, there are examples in the literature where it is properly estimated: in [22] a group of non-linear observers based on Dugoff's tyre model and vehicle dynamics are employed relying on longitudinal, lateral acceleration, yaw rate and steer angle measurements. Another approach is reported in [23] where a cascade of observers system is employed for longitudinal and lateral velocity estimation. In the current study, longitudinal velocity is assumed to be obtained either from an estimation process or measured from a GPS unit directly, that provides an acceptable accuracy for the proposed implementation.
The challenge of using the same model for the feedback controller and the EKF (with the only addition of u) is represented by the choice of the internal model inputs. The MPC controller calculates the rate of variation of longitudinal normalized forces on both vehicle axles and these outputs correspond exactly to the Kalman filter model inputs. It is thus clear how the EKF and the MPC need to be considered as a single integrated control entity. An additional assumption is also adopted in the estimation process: since a braking event on standard high friction asphalt condition is considered, it is reasonable to assume that the normalized longitudinal forces μ_R, μ_F both at the front and rear axle results bounded in the open interval $(0, 1)$. States constraints in the estimation has been applied with different level of complexity in the literature: an example where the sigma points are projected in the feasible region for an Unscented Kalman Filter can be found in [24], or in the case of the Extended Kalman Filter this projection is known as clipping [25]. A similar technique is adopted in our study by means of a saturation on the predicted states corresponded to μ_R, μ_F of the Kalman Filter internal model. In this sense the saturation is not applied on the estimated states, but they can still be corrected by the kalman filter, although we lose estimation optimality properties because of the saturation.
A more elegant solution would be the Moving Horizon Estimation (i.e. MHE) where con-

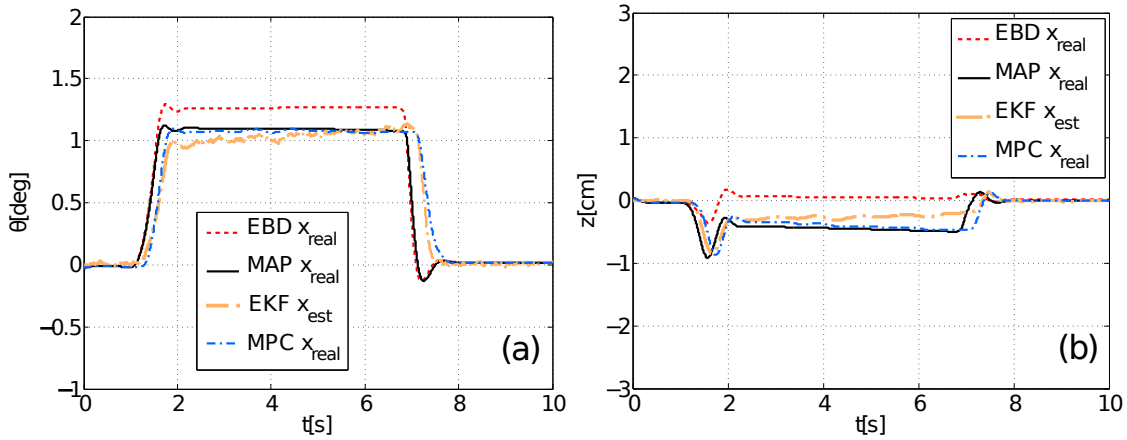

Figure 4. Comparison of (a) pitch angle and (b) heave between simulations for a 0.5g step-input deceleration, employing EBD strategy (red-dashed line), MAP (black-solid line) and MPC (blue-dashed-dotted line) in a high fidelity environment. Estimated variables are also reported (orange-dashed-dotted line).

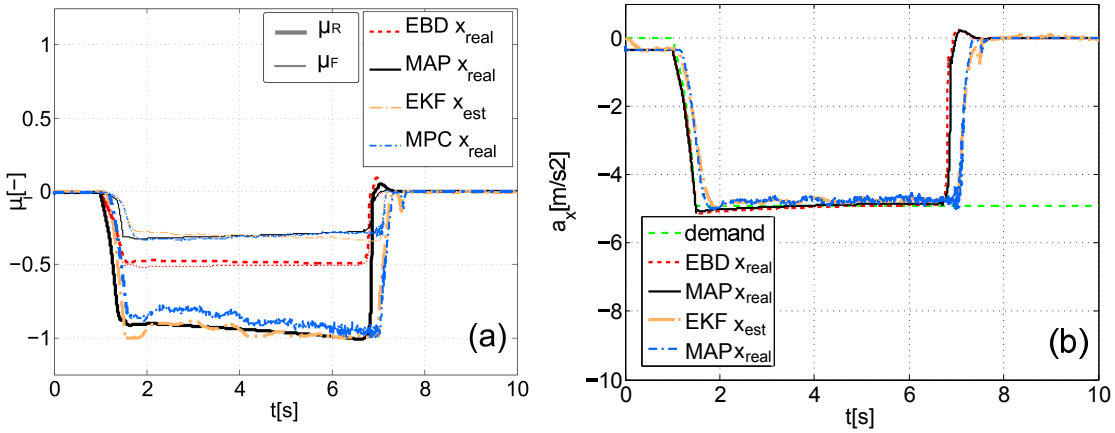

Figure 5. Comparison of (a) normalized longitudinal forces (thick line for rear and thin line for front) and (b) longitudinal acceleration between simulations for a 0.5g step-input deceleration, employing EBD strategy (red-dashed line), MAP (black-solid line) and MPC (blue-dashed-dotted line) in a high fidelity environment. Estimated variables are also reported (orange-dashed-dotted line).

straints are included in the estimation process, but this option has been discarded for its limitations in terms of computational effort [25]. A survey of solutions to the constrained estimation can be found in [26].

5. MPC IN HIGH FIDELITY MODEL SIMULATIONS AND EKF ESTIMATION

In this section we present simulation results of the MPC-EKF controller developed above, using the high fidelity vehicle software CarMaker from IPG®. Tyre models, tyre and suspension compliance derived from measurement of the real vehicle as well as aerodynamics features are all included to explore the issues that the implementation of the proposed MPC strategy would lead to. The controller is compared against the EBD and Quasi-static optimal map from [15], which we note are feed-forward algorithms mapping acceleration demand to brake force distribution.

One of the challenges in applying such a control system to a realistic vehicle model is how to manage the controller outputs, thus the inputs of the system. As explained

in section 3 the MPC outputs rate of variation of normalized longitudinal forces for front and rear axles. In order to apply these control actions to the plant a few steps are necessary: the MPC outputs are first integrated in order to obtain normalized longitudinal forces and are then multiplied by their respective front and rear vertical forces calculated employing a quasi-static condition of constant deceleration for every case of the measured longitudinal acceleration (available from the installed sensors). In this way the feedback controller needs to cope with an external injection of noise and thus its robustness needs to be addressed with a proper fine tuning. For this MPC formulation a set of hard constraints is defined both for input and longitudinal forces states (equations (30) and (29)) in order to avoid non realistic build-up times on one hand and to consider only feasible braking actions on the other hand. For this implementation a time step of 50ms and an horizon of 150ms are selected.
As discussed previously, the MPC controllers that have been developed require full state feedback. For this reason the estimation approach presented in section 4 is adopted.
For the implementation of the EKF a time step of 5ms has been finally employed. The selected scenario for this test include a single braking event from the initial velocity of 100kph with a deceleration level demand from the driver of -0.5g. Figure 5b shows how the demand builds up in 0.5s from zero to the predefined value (i.e. corresponding to a specific brake pedal stroke) and is held until the end of the simulation also beyond the point where the vehicle comes to a full stop. The driver is not modulating in any way the braking effort on the pedal.
Figure 4a shows as the pitch angle is reduced with respect to EBD. A comparison with results employing the quasi-static map shows how the strategy in terms of force distribution is the same (Fig.5a), and thus leads to the same values in terms of pitch and heave vehicle motions (Fig.4a-b). It has to be noticed how the introduction of constraints on the inputs results in a slightly delayed achievement of the pitch angle for the deceleration level target (Fig.4a). In the last part of the manoeuvre the controller is switched from $\mathrm{MPC_{mp}}$ to $\mathrm{MPC_{fs}}$. This last controls longitudinal forces at a high rate of variation reducing both front and rear braking action and thus the vehicle acceleration. Since the full-stop strategy is applied on the minimum pitch distribution, in this particular case it results in a strategy where the front normalized force is cancelled before the rear one that leads the vehicle to smooth a full-stop without any pitch rebound. The MAP strategy is once more affected by this phenomenon, as per the EBD case.
Some discrepancies (between MPC-EKF and MAP) are present for the rear normalised braking force, whereas the front one is exactly the same. This translate in a negligible difference in terms of deceleration (Fig.5b), with almost no effects on the pitch and heave values. Small errors in the longitudinal normalised forces estimation (and correspondingly in the pitch angle and heave) are recorded and shown in Fig.4-5. As already mentioned the EBD as well as MAP strategies are feed-forward approaches, where the aerodynamic force is not accounted for, this act as an external decelerating force that makes the vehicle to stop slightly before the MPC-EKF controlled one. The difference in deceleration level is negligible for any pitch angle effect.

Braking distance analysis

Regarding the braking distance, it has to be notice that there could be two main causes to obtain different values: the first aspect is the reactivity of the control strategy. It has already been discussed how the MPC-EKF controller reacts slightly slower than the

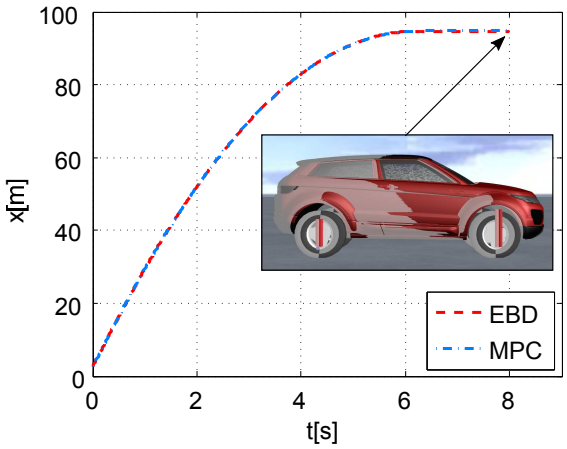

Figure 6. Braking distance comparison between EBD (red-dashed line) and MPC-EKF(blue-dashed-dotted line) for a braking manoeuvre of 0.5g longitudinal deceleration and initial speed of 100kph.

EBD one, but since the proposed strategy is to be applied for low/medium deceleration level, and not for emergency braking, this delay can be compensated by the driver than will adapt his driving style and braking to the specific controller, like he would do with a new car. The second important aspect, that has to be considered is the intervention of the second feedback controller for the full-stop strategy. As already mention in order to reduce the pitch rebound, the deceleration has to be decreased in the final part of the braking manoeuvre, and this will necessary lead to an increase of the braking distance, but since this regulation happens below the threshold of 1kph, the effect on the braking distance turns out to be negligible, as clearly shown in Fig.6. In this case the same scenario of braking with a commanded deceleration level of 0.5g from an initial speed of 100kph is considered. To isolate the effect of the full-stop strategy, the brakes' dynamics for the EBD case is customised in order to obtain the same build-up time than for the MPC case. The difference in the braking distance results being far less than a wheel radius, thus the full-stop strategy can be applied without any concern with this regard.

Driver comfort in the full-stop braking

Regarding the full-stop event, the reason of the discomfort finds for sure one of its causes in the chassis pitch rebound itself, but it arises also from the combination of the different accelerations that the driver is exposed to. Accelerations at the driver's head are of particular concern when driving comfort is involved. An analysis of longitudinal and vertical accelerations, that are projected from the vehicle centre of gravity (where they are measured) to a point that coincides with the position of the head of a driver of average height, is carried out. Figure 7a-b presents the results for the same braking scenario already employed in the braking distance analysis. In Fig.7a the last part of the braking manoeuvre, when the vehicle comes to a full-stop, is reported in terms of longitudinal acceleration at the head point: for the EBD case, the driver first fully recovers the deceleration, then undertakes a peak of positive acceleration of 0.5m/s2 while the pitch angle starts to be recovered, the MPC control action is able to fully damp any positive peak of acceleration in the forward direction, the negative one shown in the figure is only due the vibration in the control action, already mentioned throughout the paper. However, more interesting effects are recorded if the acceleration in the vertical direction is considered (Fig.7b). The EBD case, exhibits a peak of acceleration of around 0.75m/s2

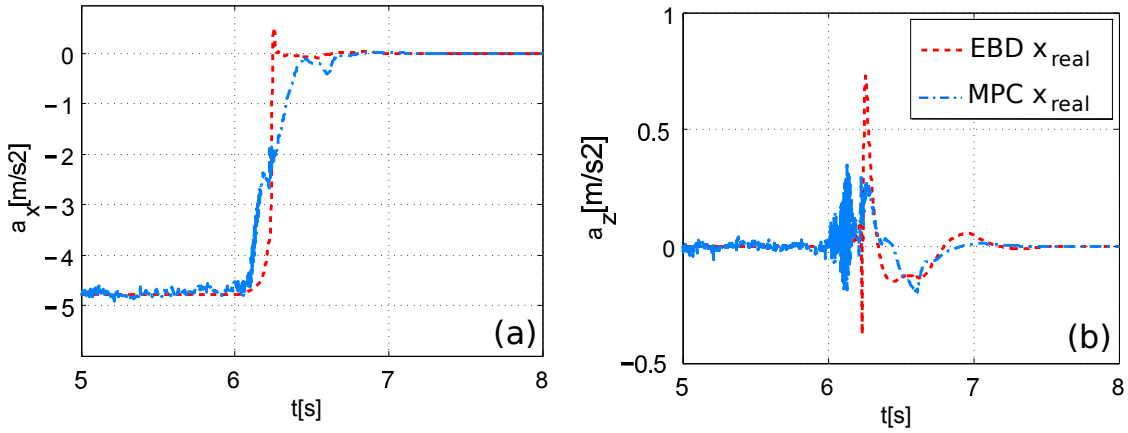

Figure 7. Comparison between EBD (red-dashed line) and MPC (blue-dashed-dotted line) in terms of (a) longitudinal acceleration and (b) vertical acceleration calculated at the driver's head point. The results show much lower values for the MPC case employing the full-stop control strategy.

for the vehicle stop followed by a -0.15m/s2, that corresponds to the pitch recovery and a small 0.05m/s2 for the rebound. The MPC controlled vehicle instead, after some vibrations just after t=6s, exhibits a first proper peak of about 0.30m/s2 (thus 60% lower than for EBD) followed by a negative peak of around -0.2m/s2 again due to the control action vibration at the very end of the manoeuvre. The peak for the pitch rebound is, in this case, completely cancelled. From this simple analysis it is clear that the improvement for the driver feel provided by the full-stop strategy is of paramount importance and it comprehends more than what is visible from the vehicle pitch measurement. The pitch rebound is a consequence of the hard (i.e. non smooth) full-stop that leads to peaks of acceleration at the driver's head, and it has been demonstrated that, concentrating on cancelling this phenomenon is possible to increase the driver comfort.

Driver-in-the-loop scenario

The MPC-EKF integrated controller is now tested, together with the feed-forward MAP strategy, on a realistic braking event from the speed of 30m/s employing a driver-in-the-loop approach generating the acceleration demand input by means of a driving simulator controller. This strategy allows to test controller and estimation reaction at different inputs amplitudes and frequencies. In order to obtain the best performance of the controller, for different conditions of deceleration demand from the driver, two major adjustment are applied to the state target weight matrix Q: the weight on pitch target is increased while moving to lower deceleration demand (linear function), in this way the pitch angle will be minimised whilst achieving the demanded acceleration. Furthermore, the weight on the acceleration target is maintained on a low value until the error between acceleration state and target becomes lower than a specific threshold $a_{x_{th}}$ =0.25g, then it is increased to force the vehicle to remain in the desired deceleration condition. Results for the driver-in-the-loop scenario are reported in Fig.8. They include different deceleration demands in the range of operation of the minimum pitch strategy (medium to low deceleration levels). When implementing the MAP brake force distribution on this scenario, the limitations of the feed forward approach become evident. For medium deceleration level the demanded deceleration from the driver is achieved with good accuracy, whereas moving towards low deceleration levels the brake distribution in use is delivering higher longitudinal negative acceleration than the demanded. The reason of this is

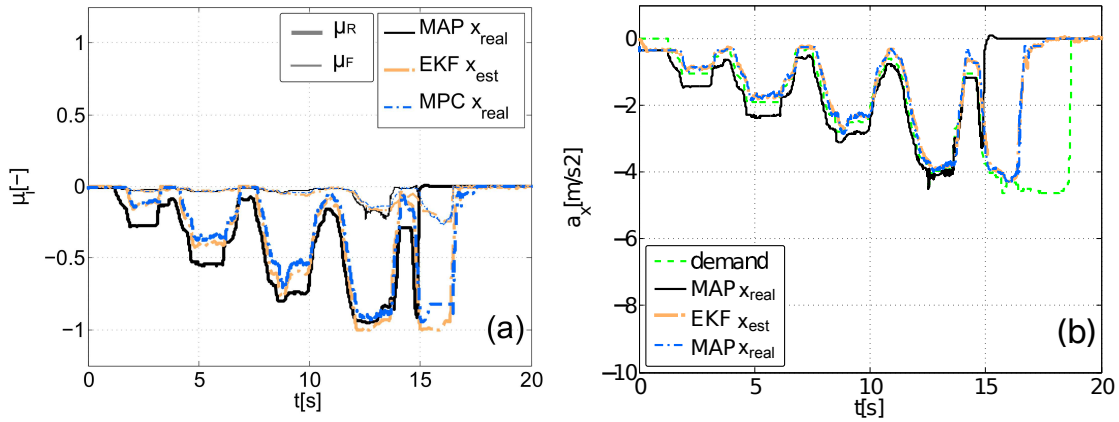

Figure 8. Comparison of (a) normalized longitudinal forces and (b) longitudinal acceleration between simulations for a realistic braking scenario, employing MAP (black-solid line), MPC (blue-dashed-dotted line) and EKF estimated variables (orange-dashed-dotted line) in a high fidelity environment.

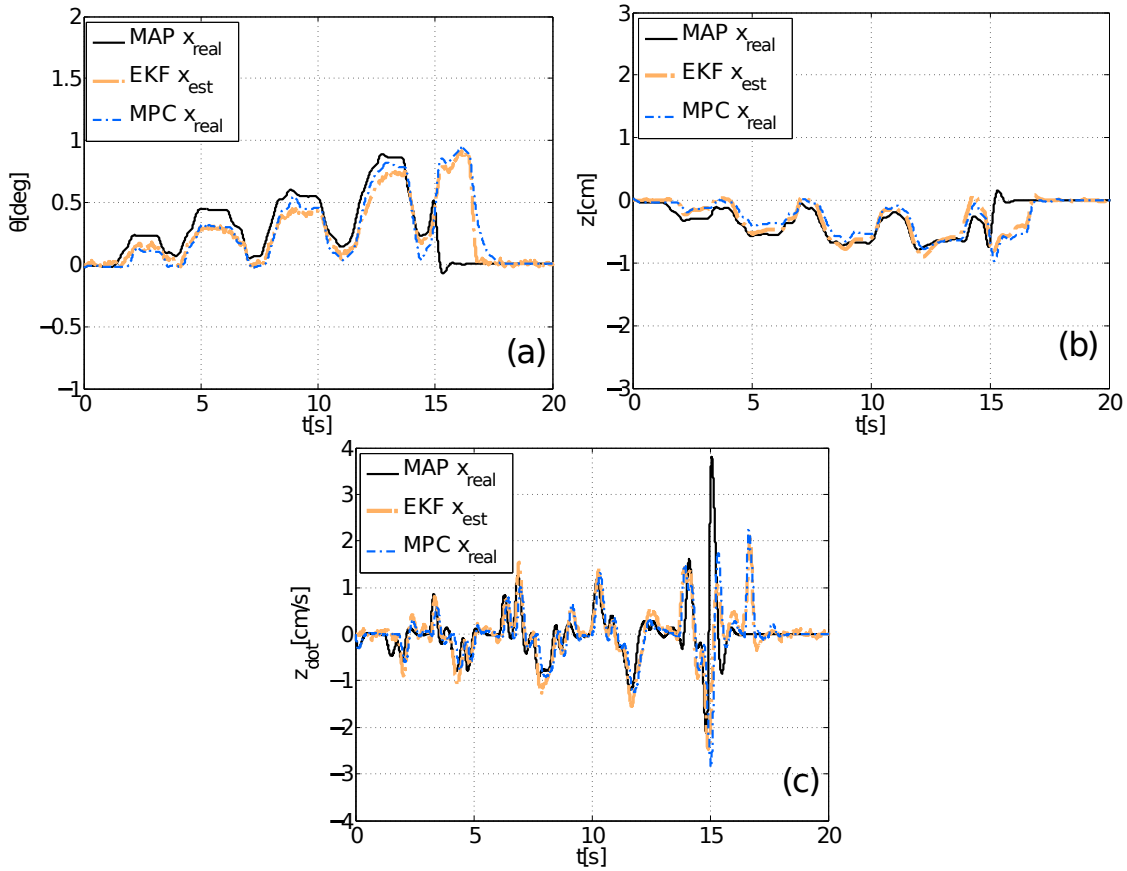

Figure 9. Comparison of (a) pitch angle, (b) heave and (c) heave rate between simulations for a realistic braking scenario, employing MAP (black-solid line), MPC (blue-dashed-dotted line) and EKF estimated variables (orange-dashed-dotted line) in a high fidelity environment. Gain scheduling is applied.

on one side the presence, in the first part of the braking scenario, of a fairly important aerodynamic force that becomes predominant over the friction brake action and that it is not accounted for in the quasi-static study. On the other side the dynamic model, used to generate the brake force map, includes simplifications in the motion of the centre of gravity and in the wheelbase variation during braking that affect both front and rear

vertical forces and thus longitudinal forces generation as well. Although the deceleration results slightly different from the demand, the trend for the brake force distribution is absolutely clear and follows a strategy with a brake force biased to the rear, until the front brake force is necessary to achieve the demanded deceleration level. Observing the MPC results in Fig.8b it is clear how the feedback controller is able to track much more closely the demand from the driver, unless the frequency on the brake pedal exceeds the feasible limitations for the MPC controller (limits on the rate of variation of longitudinal forces). Figure 8a shows how the demand is achieved imposing a brake force distribution that follows the same trend generating by the MAP strategy, with a perfect match for the case where both MAP ad MPC are delivering the same vehicle acceleration. From the estimation point of view, the EKF provides a fairly accurate feedback signals to the MPC controller in terms of front and rear normalized longitudinal forces. Figure 9 reports other important information about the estimation process. In can be noticed how, for all the systems states, the match between the real ones represented by MPC and EKF estimated ones is accurate enough, with minor discrepancies in the pitch and heave states. In particular, it is important to underline how even if the pitch angle (Fig.9a) in the very last part of the manoeuvre is slightly underestimated, the MPC_{fs} is still able to calculate the control action to lead the vehicle to a smooth full stop.
The estimation of the vehicle pitch angle, heave motion and heave rate presented in Fig.9b-c represents a novelty in the literature, with regards to model based estimation and could be employed for other applications in the future, to control the chassis motion of a vehicle through feedback approach. The last point is that, while assessing the effectiveness of the estimation, we must remember that the inputs for the Kalman filter internal model are taken directly from the output of the MPC controller and not from the vehicle itself, so that the estimation part could potentially destabilize the control one and vice versa. This is not happening for our controller, even in a realistic varying scenario as the one presented.

6. BRAKE FORCE DISTRIBUTION AND LATERAL VEHICLE DYNAMICS INTERACTION

Shifting the braking effort towards the rear axle does not have an effect only on the pitch-heave motion, but also the handling characteristics of the vehicle are affected. The reason is the well-known coupling effect between longitudinal and lateral tyre-ground interaction forces on each corner of the vehicle. In other words, increasing the tyre utilisation in the longitudinal direction will generate a decrement of the lateral capability in a nonlinear way.
As already mentioned, the current strategy is considered to be designed for a vehicle equipped with widespread safety systems such as ABS and ESP, in order to reduce the chance of instability while braking into a turn and preserve the braking capability. In particular, although even for medium/ high deceleration levels no rear wheel locking has occurred in the straight line scenario, when the vehicle has to be decelerated in a corner, the chance of the inner wheels, in particular the rear one, to lock is much higher.
A low level controller able to maintain the longitudinal wheel slip below a certain threshold is in this case necessary, on one side for the aforementioned instability risks, and on the other hand to obtain the best performance of the MPC-EKF controller, that could lead to non optimal results. This last aspect is mainly due to the fact that the observer (EKF) internal model does not include the lateral dynamics and lateral load transfer, so that when the braking action lead one of the wheel to decelerate much more

than the others, estimations errors may occur and the results, even tough still capable of delivering the demanded deceleration level, will not be pitch-optimal any more. In order to assess the worst case scenario, when systems such as ABS and ESP are not present on the vehicle, a set of high fidelity model simulations are performed in mixed longitudinal-lateral dynamics manoeuvres. In Fig.10 the case of a braking into a turn manoeuvre is presented. The scenario is a left turn from an initial velocity of 77kph and a fixed steering wheel angle input of 30deg, that lead to an initial lateral acceleration of 4m/s2. After one second the deceleration level demand is varied from zero to 3m/s2. The cases of EBD and minimum pitch brake distribution (MPC-EKF) are compared.
As soon as the braking command is elaborated, the MPC-EKF controller delivers a braking pressure distribution that is in line with the expectations (Fig.10b-c), with a very low pressure at the front and high pressure at the rear wheels. Since the controller is only based on longitudinal dynamics, the distribution for left and right sides of the vehicle is exactly the same. At this point due to the longitudinal and lateral load transfer combination the rear inner (left) tyre results to be much more utilised than the other three, as it is reported in Fig.10f, where the rear left tyre slip ratio stays on high values, meaning that the wheel is much harder decelerated, between t=1.5s and t=4s. An average utilisation both for the front and the rear tyre is shown in Fig.10g together with the estimated quantities (computed with the EKF that does not account for lateral load transfer).
It may appear that the estimation error could cause serious problem to the control strategy, but in reality the unaccounted lateral load transfer does not affect the controlled pressures. The estimated normalised forces quantities are correctly computed for the longitudinal dynamics that is imposed on the vehicle, but due the lateral load transfer results different than the real one, this means that the pressure command that are delivered are the same as if the braking manoeuvre was performed on a straight road. Observing the real non-normalised longitudinal forces on the two sides of the front and rear axle (Fig.10d-e) it is possible to isolate the effect of the lateral load transfer on the force distribution. Between t=1s and t=1.5s, while the braking action builds up, the effective force distribution is the expected one, with most of the braking effort carried out by the rear tyres, then between t=1.5s and t=2s the rear lateral forces are reduced due to the longitudinal engagement and this results in an oversteering behaviour of the vehicle and thus an increase of the level of lateral acceleration that reaches a peak of about 5.5m/s2. This further increases the lateral load transfer and make the rear inner wheel to decelerate more. In this process the combination of vertical loads and tyre longitudinal coefficients μ_i generate a non-normalised force distribution that replicate exactly the one realised with the EBD distribution (between t=2s and t=3s), in this way the oversteer behaviour is mitigate, but this is done at the expanses of optimality in the pitch minimisation distribution, that in this situation becomes anyway of secondary importance. Thank to the velocity drop, the lateral acceleration is reduces below a level that permits all the four wheels to spin at a similar rotational speed again (around 3m/s2 at t=4s), without tyre saturation (Fig.10g), and the effective force distribution returns on the expected values, thus biased to the rear axle (Fig.10d-e).
The combination of forces on the four wheels, together with the fixed steer command determine the trajectory of the vehicle. Figure 10h shows how up to t=3s the trajectory of the centre of gravity between the vehicle employing EBD and the one adopting the minimum pitch distribution is the same. When the braking action is then transfer to the rear, the vehicle equipped with the feedback controller shows the oversteer behaviour and tights its trajectory with respect to the EBD equipped one. It has to be noticed that, by the time the vehicles' trajectories start to diverge, the velocity has dropped to a value of 57kph, that still correspond to a lateral acceleration of about 4m/s2, and thus the

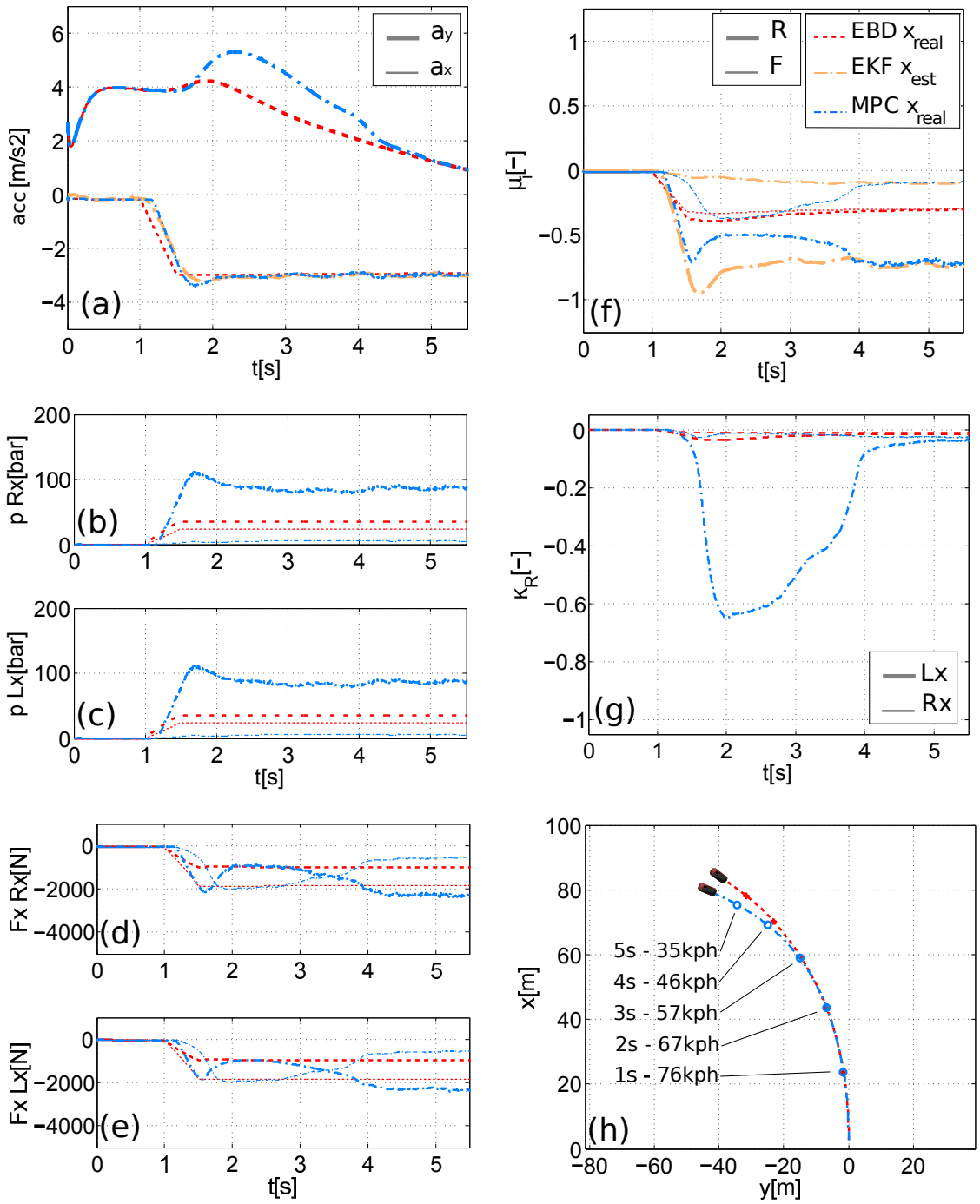

Figure 10. Comparison between EBD (red-dashed line), MPC (blue-dashed-dotted line) and EKF estimation (orange-dashed-dotted line) for a braking into a left turn manoeuvre at the initial lateral acceleration of 4m/s2, initial speed of 77kph and fix steer wheel angle of 30deg in terms of (a) longitudinal and lateral accelerations, (b) commanded braking pressure on both wheels of the right side and (c) left side, (d) non-normalised longitudinal forces on both tyres of the right side and (e) left side, (f) average normalised forces for both axles, (g) rear tyres longitudinal slip ratio for the right and left sides, (h) vehicle trajectories with indication of manoeuvring time and corresponding longitudinal speed.

stability of the vehicle is proved to be maintained even for fairly aggressive manoeuvre. It has to be remarked that this behaviour could not probably be acceptable for a production vehicle and thus the aforementioned ABS and ESP systems will have to be in place,

but this will be also the case for the EBD strategy, that as the minimum pitch one, is only based on calculation of the longitudinal load transfer, and will eventually lead to wheels lock simultaneously at the front and rear axle on the same inner side, for more aggressive manoeuvres or low adhesion surfaces. This will lead even in the case of the 'ideal' distribution to an hazardous situation that has to be mitigated, like clearly shown in [7]. In the same paper is reported how moving to low adhesion conditions the only ESP intervention (based on vehicle sideslip angle) may not be enough, so two solution are proposed to address this problem. The first one is to vary the brake distribution when one of the rear wheel exceed a certain threshold of longitudinal slip: this approach was thought for regenerative braking at the rear axle, deactivating the extra braking action when required. The second one implies the use of a centre locking between the front and rear axle, to redistribute the braking effort (with a torque split similar to the 'ideal' one) amongst front and rear wheels. This solution anyway may affect the performance of ESP and ABS systems and leads to other technical issues reported in the paper.
Another way to mitigate the oversteering behaviour due to the decrease of rear lateral forces has been proposed in [14], where the brake force distribution biased to the rear is applied only on the outer wheels in order to counterbalance the destabilising yaw moment due to the inner wheel poor lateral capability. This solution could be applied to the system proposed in this paper to reduce the risk of wheel locks and thus further reduce the intervention of ABS and ESP safety systems.

7. CONCLUSIONS

In this paper, we addressed the problem of controlling the pitch angle of a vehicle during braking, actively varying the brake force distribution. In the current study the problem has been solved employing an MPC strategy with good results that have been compared with a previous research solution based on a quasi-static map. Employing full-state feedback controllers allowed us to add an acceleration control to the pitch and heave control action.
The problem of a hard full-stop and the pitch rebound has been also addressed by means of the same feedback controller, varying weight matrices below a predefined vehicle speed threshold. The proposed solution has proved to be capable of providing a smooth stop of the vehicle to improve driver comfort (in terms of pitch rebound cancellation and accelerations at the driver's head point), without affecting the braking distance.
Adopting the same internal model as for the feedback controllers, an extended Kalman filter state observer has been developed and integrated together with the MPC controller to provide the necessary state feedback, including pitch angle, heave motion and rate that are almost absolute novelties for estimation in the literature. Simulation in a high fidelity environment revealed the effectiveness and robustness of the state observer as well as the effectiveness of the MPC controllers in both real driving scenarios and the single case study, in terms of target acceleration tracking and pitch reduction both during the braking event and the full-stop case. Although the presented system has been considered for implementation in combination with widespread safety system such as ABS and ESP, a worst case scenario of a braking into a turn manoeuvre employing a vehicle devoid of such safety features, was considered and analysed in details. Results shows how, although the optimality of the strategy is affected by an unaccounted lateral load transfer, the control action is still acceptable and guarantees a certain level of vehicle stability for mid aggressive manoeuvres. The aforementioned systems has to be in place when considering production vehicles driving on public roads.

Funding

This work is undertaken within the Evoque_e project, co-funded by the UK's innovation agency, Innovate UK.

References

[1] Rill. Road vehicle dynamics fundamentals and modelling. Boca Raton, FL, USA: CRC Press, Taylor and Francis Group; 2012.
[2] Anonymous. Safety, comfort and convenience systems: Function, regulation and components. Cambridge, MA, USA: Robert Bosch GmbH, Bentley Publishers; 2006.
[3] Chu L, Mingli S, Fang Y, Guo J, Zhou F. Braking force distribution strategy for hev based on braking strength. In: 2010 International Conference on Measuring Technology and Mechatronics Automation (ICMTMA); March 13-14. Changsha City; 2010.
[4] Guo J, Wang J, Cao B. Application of genetic algorithm for braking force distribution of electric vehicles. In: 4th IEEE Conference on Industrial Electronics and Applications; May 25-27. Xian; 2009.
[5] Zhang Z, Xu G, Li W, Zheng L. Regenerative braking for electric vehicle based on fuzzy logic control strategy. In: 2nd International Conference on Mechanical and Electronics Engineering; August 1-3. Kyoto; 2010.
[6] Paul D, Velenis E, Cao D. Tire-road-friction-estimation-based braking force distribution for awd electrified vehicles with a single electric machine. In: IEEE International Conference on Sustainable Energy Engineering and Application (ICSEEA); October 5-7. Bandung; 2015.
[7] Hancock M, Assadian F. Impact of regenerative braking on vehicle stability. In: IET The Institution of Engineering and Technology Hybrid Vehicle Conference; December 12-13. Coventry; 2006.
[8] Campos J, Davis L, Lewis F, Ikenaga S, Scully S, Evans M. Active suspension control of ground vehicle heave and pitch motions. In: 7th IEEE Mediterranean Conference on Control and Automation; June. Haifa; 1999.
[9] Margolis D. Semi-active heave and pitch control for ground vehicles. Vehicle System Dynamics. 1982;11(1).
[10] Gillespie T. Fundamentals of vehicle dynamics. Warrendale PA USA: Society of Automotive Engineers SAE International; 1992.
[11] Milliken W, Milliken D. Race car vehicle dynamics. Warrendale PA USA: Society of Automotive Engineers SAE International; 1995.
[12] Wang X, Shi G, Jin L, Ying G, Yang H. A study on pitching charactersitics of the passenger car in braking process. In: Proceedings of the FISITA 2012 World Automotive Congress; November 27-30. Beijin; 2012.
[13] Danesin D, Krief P, Sorniotti A, Velardocchia M. Active roll control to increase handling and comfort. SAE Technical Paper; 2003. Report no.:.
[14] Morita T, Matsukawa T. Improvement of vehicle dynamics by rear braking force control. Vehicle System Dynamics. 1995;24(4-5):401–412.
[15] Tavernini D, Velenis E, Longo S. Model-based active brake force distribution for pitch angle minimization. In: Decision and Control (CDC), 2015 IEEE 54nd Annual Conference on. IEEE; 2015.
[16] Sato S, Fujimoto H. Proposal of pitching control method based on slip-ratio control for electric vehicle. In: Proc. Proc. The 34rd Annual Conference of the IEEE Industrial Electronics Society, Florida; 2008.
[17] Lee JH, Ricker NL. Extended kalman filter based nonlinear model predictive control. Industrial & Engineering Chemistry Research. 1994;33(6):1530–1541.
[18] Bellemans T, De Schutter B, Wets G, De Moor B. Model predictive control for ramp metering combined with extended kalman filter-based traffic state estimation. In: Intelligent Transportation Systems Conference, 2006. ITSC'06. IEEE. IEEE; 2006. p. 406–411.
[19] Eric Tseng H, Xu L, Hrovat D. Estimation of land vehicle roll and pitch angles. Vehicle System Dynamics. 2007;45(5):433–443.
[20] Van Loan C. Computing integrals involving the matrix exponential. 1978;AC-23(3):395–404.
[21] Welch G, Bishop G. An introduction to the kalman filter. 2006. University of North Carolina: Chapel Hill, North Carolina, US. 2006;.

[22] Zhao LH, Liu ZY, Chen H. Design of a nonlinear observer for vehicle velocity estimation and experiments. 2011;19(3):664–672.
[23] Li L, Song J, Kong L, Huang Q. Vehicle velocity estimation for real-time dynamic stability control. International journal of automotive technology. 2009;10(6):675–685.
[24] Kandepu R, Imsland L, Foss BA. Constrained state estimation using the unscented kalman filter. In: Proceedings of the 16th Mediterranean Conference on Control and Automation. Citeseer; 2008. p. 1453–1458.
[25] Haseltine EL, Rawlings JB. Critical evaluation of extended kalman filtering and moving-horizon estimation. Industrial & engineering chemistry research. 2005;44(8):2451–2460.
[26] Simon D. Kalman filtering with state constraints: a survey of linear and nonlinear algorithms. IET Control Theory & Applications. 2010;4(8):1303–1318.